Iranian Journal of Chemical Engineering

Journal Homepage: www.ijche.com

pISSN: 1735-5397
eISSN: 2008-2355

Effect of Magnet Position on the Flow and Thermal Performance of Ferrofluids in a Channel with Constant Wall Heat Flux: A CFD Study

Masoud Taheri, Mahdieh Abolhasani*, Maryam Dinarvand

Faculty of Chemical, Petroleum and Gas Engineering, Semnan University, Semnan, Iran

ARTICLE INFO

Article type:
Research article

Article history:
Received: 2025-09-10
Revised: 2025-10-15
Accepted: 2025-11-4
Available online: 2025-11-22

Keywords:
Magnetic field,
Ferrohydrodynamics,
Magnet position,
Kelvin force,
Heat transfer,
Fe_3O_4/water ferrofluid

ABSTRACT

This study presents a numerical investigation into the influence of the magnet position and its distance from the channel inlet on the heat transfer and flow behavior of ferrofluid (FF), including Fe_3O_4/water flowing through a horizontal channel under a constant wall heat flux. Three magnet positions were considered—at the inlet, middle, and outlet of the channel—to identify the best configuration to enhance the heat transfer. Permanent magnets with a remanent magnetic flux density of 0.4 T were modeled. The nanoparticle concentration was 5 Vol.%, and the Reynolds number was 100. The effects of magnet position on the local magnetic flux density, Kelvin force, streamlines, velocity and temperature distributions, and Nusselt number (Nu) were investigated. The problem was solved by assuming incompressible, laminar, and steady-state flow. The Galerkin weighted residual finite element method was used to solve the governing equations simultaneously. Results revealed that when magnets were positioned at the inlet or outlet, the magnetic field effects were localized and produced minimal impact on the flow and temperature fields. Conversely, when the magnets were located in the middle of the channel, the most substantial magnetic field gradients and Kelvin forces were generated, which created recirculation zones and increased fluid mixing, resulting in a more uniform temperature distribution, a significant enhancement in the local Nu and an average Nu of 5.31. Finally, this study proposes placing the magnet in the middle of the channel as the most effective configuration for enhancing the convection heat transfer.

DOI: 10.22034/ijche.2025.545788.1571 URL: https://www.ijche.com/article_234721.html

*Corresponding author: m.abolhasani@semnan.ac.ir

1. Introduction

The demand for effective thermal management solutions has increased in recent years due to the rapid development of microelectronic technologies, resulting in higher heat generation and increased power densities. Various design strategies, materials, and cooling techniques used in microelectronic devices have become increasingly important to improve heat dissipation and maintain temperature uniformity. By analyzing recent advances and challenges, the importance of optimizing the performance of microelectronic devices has increased to ensure the functionality and efficiency of electronic devices [1,2]. In this regard, various methods, such as the installation of blades and the addition of phase change materials, showed significant heat dissipation [3,4].

With the development of nanotechnology in recent years, nanofluids (NFs), due to their superior thermal properties compared to conventional coolants, are being used to enhance heat dissipation. The presence of nanoparticles (NPs) in the base fluids affects their thermophysical properties [5]. NFs provide more efficient and reliable thermal management solutions for high-performance electronic systems [6]. By increasing power and heat generation in electronic chips, efficient cooling methods, such as using NFs, are becoming increasingly important. NFs have better heat dissipation in electronic equipment due to their higher thermal conductivity than conventional pure fluids. NFs are of great interest due to their unique properties and have numerous applications in different industries and fields such as the electronics industry, thermal engineering, and bioengineering [7,8].

A class of NFs called ferrofluid (FF), which is composed of a suspension of magnetic NPs, has garnered significant interest due to its distinctive characteristics [9,10]. When FFs are exposed to a magnetic field (MF), they behave differently from conventional fluids that remain unaffected by such fields. Their interaction with the field generates a Kelvin force, endowing the FF with distinctive properties. This phenomenon has sparked interest in a field of study known as Ferrohydrodynamics (FHD), which finds applications across various domains [11,12].

Karami et al. [13] studied the convection heat transfer within a microchannel, which was a cylindrical pit with a uniform heat flux applied to the bottom wall, under rotating and static MFs. They explored the effect of flow rate, MF induction, and NP concentration on heat transfer characteristics. The findings indicated that NF improved the heat transfer compared to DI water, and the rotating MF was more effective compared to the static MF. Cunha et al. [14] studied how FF flow in a square cavity transfers the heat when both gravity and an MF act together. They found that thermomagnetic convection increased the rate of heat transfer and that the distribution of recirculation zones was controlled by the interplay among gravitational, viscous, and magnetic forces. Mehrez and Cafsi [15] numerically studied the enhancement of the heat exchange of Fe_3O_4/water FF flow in a rectangular channel under an MF. The obtained results illustrated that the isotherms and the streamlines were significantly affected by the application of MF. They enhanced the heat exchange rate without MF by up to 20% and with MF by up to 60%.

Larimi et al. [16] studied the forced convection heat transfer of Fe_3O_4/water flow within a ribbed channel, examining various non-uniform transverse MF configurations produced by the wires carrying electric

current. In their study, a two-phase mixture model was used. The results showed that the Nusselt number (Nu) was significantly affected by the strength of MF, especially in rib regions. They also investigated the effect of MF on the pressure drop and skin friction. Benos et al. [17] studied the behavior of magnetohydrodynamic (MHD) natural convection within a porous enclosure saturated with NF. They used Cu, Al_2O_3, and TiO_2 NPs dispersed in an aqueous suspension. The obtained results indicated that an increase in MF intensity, a decrease in medium permeability, a denser NF, and an enlargement of NPs resulted in a heat transfer reduction. Soltanipour [18] employed a two-phase model for the investigation of forced convection in a uniformly heated pipe containing Fe_3O_4/water subjected to a quadrupole MF. Three primary transport mechanisms, including magnetophoresis, thermophoresis, and Brownian diffusion, were considered.

Numerical results showed that an increase in the magnetic number, particle size, and volume fraction enhanced the heat transfer, while an increase in the Reynolds number (Re) and magnetic source length decreased the heat transfer. Nessab et al. [19] numerically investigated the effect of FF jet flow and the convection heat transfer under the influence of MFs. They used six magnetic sources outside the channel, which were arranged in a staggered manner. The side walls were insulated, and the upper and lower walls were subjected to a constant heat flux. The effect of the jet inlet height, source position, and magnetic number on the flow and heat transfer was analyzed. Xu et al. [20] conducted a 2D numerical simulation to investigate the unsteady flow and heat transfer characteristics of an isothermally cooled square cylinder in a horizontal duct under a transverse magnetic field. The simulations were performed with a lithium-lead alloy working fluid. Their study demonstrated the interaction between buoyancy and magnetic forces on fluid flow and heat transfer, which is applicable to the design and optimization of magnetohydrodynamic cooling systems.

Ghafori and Dehnavy [21] employed CFD to investigate the effects of aluminum metal foam and MFs on the flow, heat transfer, and performance evaluation criterion (PEC) in a channel. They investigated the effects of the foam height ratio, magnetic field intensity, and pore diameter and reported the highest PEC. Faghani et al. [22] studied the convective heat flux generated by the fluid flow induced by the motion of magnetic NPs using CFD-DEM coupling. The results showed that as the MF strength increased, chain-shaped clusters in the magnetic fluid became more prominent. Moreover, the particle motion disrupted the hydrodynamic and thermal boundary layers of the base fluid. They also reported that a higher conductive heat flux was observed in MFs parallel to the temperature gradient compared to those perpendicular to it.

Based on the literature survey, MF has a substantial impact on FF and the ability to regulate the flow behavior and heat transfer properties of FFs. To the best of our knowledge, limited research exists on the impact of the MF position on the local temperature, velocity, Nusselt number, and Kelvin force in FHD systems.

Therefore, the main objective of this study is to control the local temperature and local heat dissipation through the CFD simulation. For this purpose, a horizontal channel with constant wall heat flux containing Fe_3O_4/water FF flow with two permanent magnets on either side was considered. The magnets were placed at different positions relative to the inlet of the

channel. In this study, the magnets themselves were also simulated, and the fluid behavior in terms of heat transfer and hydrodynamics was analyzed, and the best place for the magnet was introduced.

2. Problem description

This study investigates a horizontal channel with dimensions of 1000 mm × 10 mm, where the wall is subjected to a constant heat flux of 500 W/m². In this system, a Fe_3O_4/water FF with a concentration of 5 Vol.% was considered as the cooling fluid passing through the channel. Two magnets (dimensions: 20 mm ×150 mm) located on opposite sides of the channel establish the MF. The magnets were investigated in three different positions along the channel: the beginning, middle, and end of the channel. Figure 1 illustrates the geometry of the studied channel, and Figure 2 shows the places of the magnets along the channel.

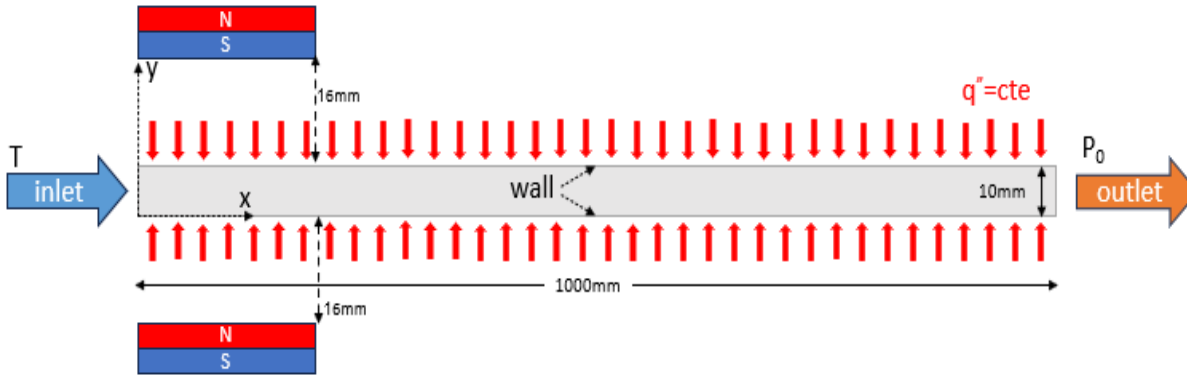

Figure 1. Geometry of the studied channel.

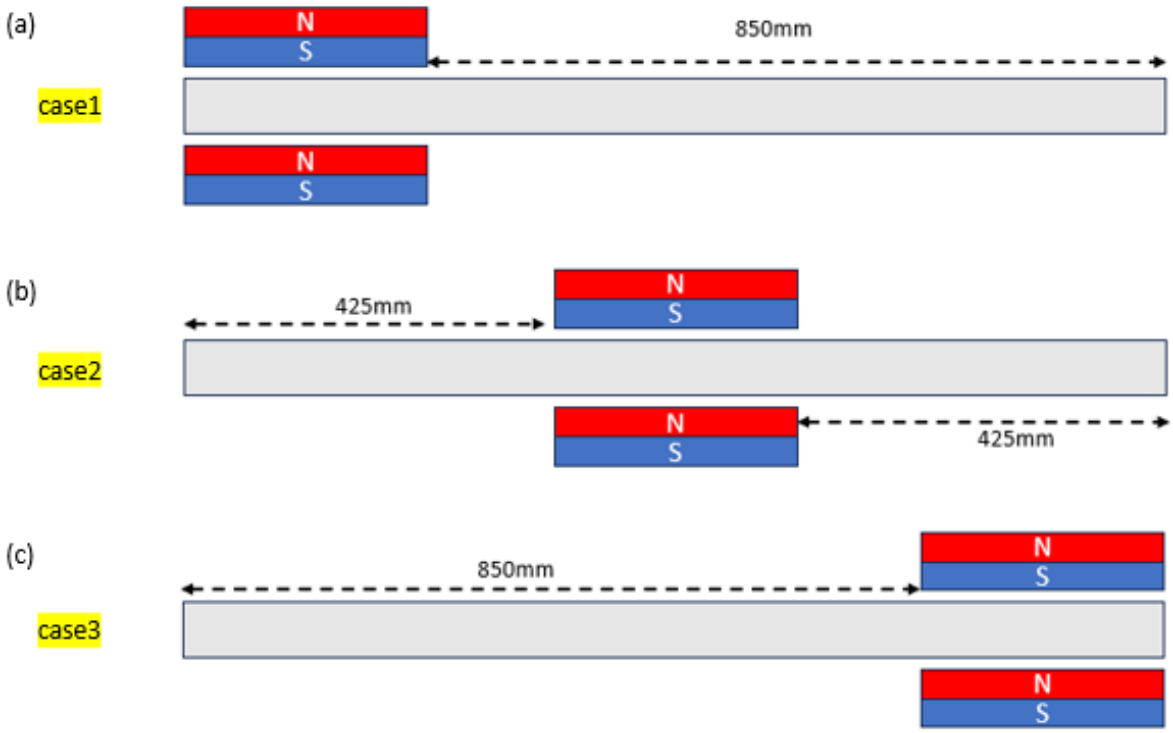

Figure 2. Magnet location and distance from the channel inlet.

3. Governing equations and boundary conditions

In this problem, the assumption of the incompressible, laminar, two-dimensional flow under steady-state conditions is considered. Given the diminutive size of NPs, homogeneous dispersion in the solution is assumed, forming a single-phase mixture; thus, the governing equations for the pure fluid are solved as follows.

Continuity equation [23,24]:

$$\rho_{ff}\nabla.\left(u_{ff}\right)=0 \quad (1)$$

The equation of motion [24,25]:

$$\rho_{ff}\left(u_{ff}.\nabla\right)u_{ff}=-\nabla.P+\mu_{ff}\nabla^2u_{ff}+F_k$$

$$F=\mu_0\,\overrightarrow{M}\cdot\nabla\vec{H} \quad (2)$$

Energy equation [24,25]:

$$\rho_{ff}\,C_{p_{ff}}\,u_{ff}.\nabla T+\mu_0 T(\frac{\partial\vec{M}}{\partial T})_{\vec{H}}.\nabla\vec{H}=K_{ff}\,\nabla^2T \quad (3)$$

The MF distribution was obtained by solving the Maxwell equations throughout all regions. The Maxwell equations are as follows [24–26]:

$$\nabla\times\vec{H}=J \quad (4)$$

$$\nabla.\vec{B}=0 \quad (5)$$

$$\vec{B}=\begin{Bmatrix}\mu_0\mu_r\vec{H}+B_r\\ \mu_0\vec{H}\\ \mu_0(\vec{H}+\vec{M})\end{Bmatrix} \quad (6)$$

where u and ρ denote the velocity and density of ferrofluids, respectively. Moreover, μ, F, and P represent the dynamic viscosity, Kelvin force, and pressure, respectively. In the energy equation, T, Cp, and K refer to temperature, specific heat capacity, and thermal conductivity, respectively. In Maxwell equations, J and B denote the electrical current density and magnetic flux density, respectively. μ_0, M, H, B_r, and μ_r are the vacuum permeability, magnetization, magnetic field, remnant magnetic flux density, and the relative magnetic permeability, respectively.

The temperature and velocity of the fluid at the inlet of the channel were T_0 and u_0, and the relative pressure at the outlet of the channel was assumed to be zero. A constant heat flux (500 W/m^2) was applied to the walls of the channel, and a no-slip condition was considered on the walls of the channel. To investigate the effect of the location of the magnets along the channel on heat transfer, the magnets were placed at the beginning, middle, and end of the channel, as shown in Figure 2. Also, B_r and Re were considered constant and equal to 0.4 T and 100, respectively. Table 1 presents the properties of the base fluid and Fe_3O_4 nanoparticles. Table 2 shows the necessary relationships for determining the properties of FF, and the boundary conditions are provided in Table 3.

Table 1.
Properties of the used nanoparticles and base fluid.

Material	$C_p\ (J/kg.K)$	$\rho\ (kg/m^3)$	$\mu\ (kg/m.s)$	$k\ (W/m.K)$
Pure water	4180	995	0.0009	0.613
Fe_3O_4 nanoparticles	670	5180	-	80

Table 2.
Relationships for calculating the properties of FF.

Properties	Equations	Reference
Density	$\rho_{ff} = \varphi\rho_{np} + (1-\varphi)\rho_{bf}$	[27]
Heat capacity	$C_{p_{ff}} = \frac{\varphi\rho_{np}C_{p_{np}} + (1-\varphi)\rho_{bf}C_{p_{bf}}}{\rho_{ff}}$	[27]
Viscosity	$\mu_{ff} = \mu_{bf}(\frac{1}{(1-\varphi)^{2.5}})$	[28]
Thermal conductivity	$k_{ff} = k_{bf}\frac{k_{np} + 2\,k_{bf} - 2\varphi\,(k_{bf} - k_{np})}{k_p + 2\,k_f + \varphi\,(k_{bf} - k_{np})}$	[29]

Table 3.
Boundary conditions.

Boundary	Conditions
Inlet: x=0	$U=U_0$, $T=T_0$
Outlet: x=1000	P=0, n.q=0
Wall: y=0, y=10	No slip, - $n.k\nabla T=q^{"}$

4. Numerical solution

The finite element method has been employed to simultaneously solve the governing equations of this problem, including the continuity equation, energy equation, and equation of motion. Moreover, the nonlinear equations were solved using the Newton-Raphson iterative method, and a convergence criterion of 10^{-6} was achieved [24,30].

4.1. Grid independence

To find a suitable mesh for solving the problem and to ensure the independence of the results obtained from the grid count, different grid numbers were examined. For this purpose, the entire computational domain was first meshed using quadrilateral and triangular elements. The obtained results are illustrated in Table 4.

Table 4.
Grid independence results at Re=100, B_r=0.4 T, and φ=0.05.

No.	Grid count	T (K)	u (m/s)	Percentage difference for T	Percentage difference for u
1	30933	299.19	0.01245	-	-
2	40761	299.17	0.012513	-0.00668	0.5060
3	53003	299.16	0.012547	-0.00334	0.2717
4	67497	299.16	0.012573	0.00	0.2072
5	83407	299.15	0.012588	-0.00334	0.1193
6	101601	299.15	0.012601	0.00	0.1032
7	122239	299.15	0.01261	0.00	0.0714

Grid independence was performed when the magnet was located in the middle of the channel, at a distance of 16 mm from the channel, Re = 100, B_r = 0.4 T, and a concentration of 5 Vol.% of Fe_3O_4 NPs. Moreover, u and T are the velocity and temperature on the center line of the channel, respectively. The comparison of the results of seven different grids in Table 4 shows that no significant change in velocity and temperature was observed as the grid count increased to more than 67497 elements.

Therefore, to reduce computational costs and run time, the grid with 67497 elements was considered the most suitable one, and other calculations and simulations were performed based on this grid. The considered computational grid is shown in Figure 3.

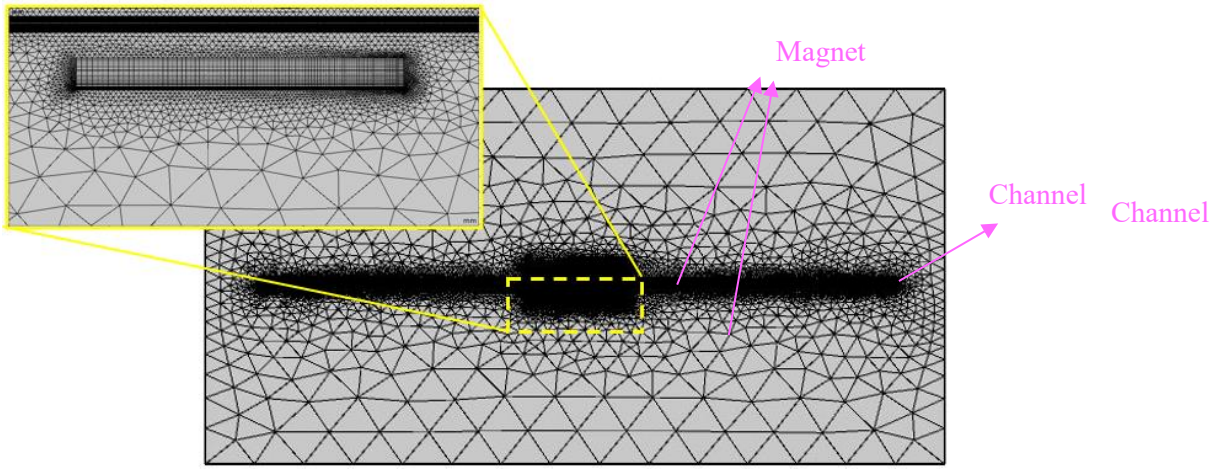

Figure 3. Mesh used in the simulation.

4.2. Validation

To validate the numerical solver and confirm the accuracy of the simulation results, the local Nu was compared with the data obtained from the studies of Dinarvand et al. [24] and Shah et al. [31] (Figure 4 (a)). The local Nusselt values were calculated for distilled water as the fluid flowing in the channel at Re=400. In addition, to check the accuracy of the simulation of magnets, the Kelvin force in the presence of the MF was calculated and compared with that in the work of Dinarvand et al. [24] (Figure 4 (b)). Therefore, the good agreement between the obtained results and those of previous works indicates the validity and high accuracy of the present simulation.

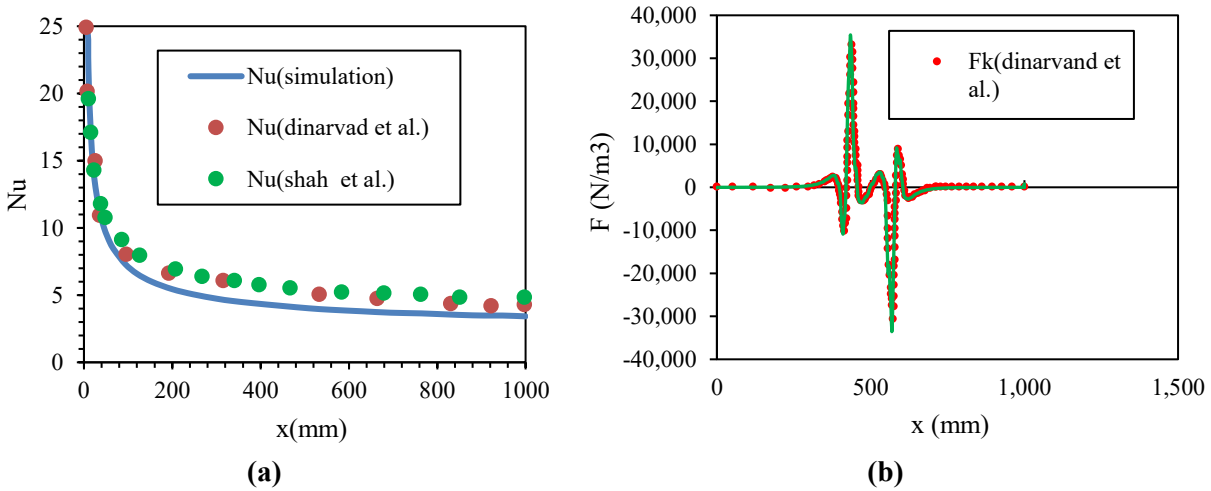

(a) **(b)**

Figure 4. (a) Comparison of the Nusselt number obtained from the present simulation with the data reported by Shah et al. [31] and Dinarvand et al. [24] for laminar water flow at Re = 400, (b) Comparison of the Kelvin force predicted by the present study with the results of the study conducted by Dinarvand et al. [24].

5. Results and discussion

In this study, the effects of the position of the magnet along the channel on the MF intensity, Kelvin force, hydrodynamic behavior of FF, and heat transfer were investigated. The simulations were conducted under the conditions of the Re =100, concentration of 5 Vol.% of NP, and Br = 0.4 T. To investigate the effect of the placement of the magnets at the beginning, middle, and end of the channel on the MF intensity and Kelvin force, two pairs of magnets were placed at different positions along the channel at an angle of zero degree to the channel. The MF lines are shown in Figure 5. In cases 1 and 3, the MF lines appear non-parallel and non-uniform, while in case 2, the field lines are almost parallel and uniform. Figure 6 illustrates the effect of the position of the magnet on the magnetic flux density (B) and the resulting Kelvin force (F). In case 1, the sharp peaks in the magnetic flux density of ~0.06 T are exhibited around the place close to the inlet, which rapidly diminish downstream, leading to strong Kelvin forces, up to ~ 2.8×10^4 N/m³, in the beginning regions. In case 2, B reaches its maximum at the middle of the channel (~0.065 T), producing pronounced positive and negative Kelvin force peaks (maximum value~3.7×10^4 N/m³), and causing significant disturbances and fluid mixing. In contrast, case 3 shows negligible magnetic flux density along most of the channel, with a localized rise at the outlet. Consequently, F is confined to the exit region, having only limited influence on the overall flow dynamics.

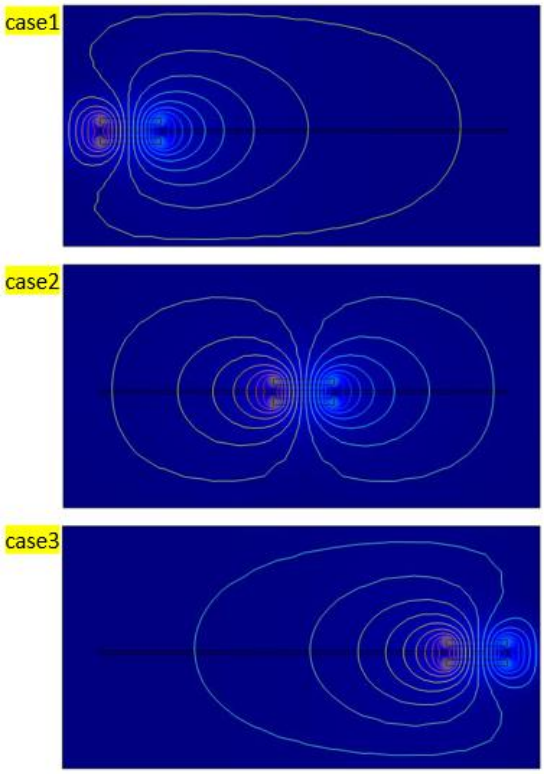

Figure 5. MF lines between two magnets in three different cases.

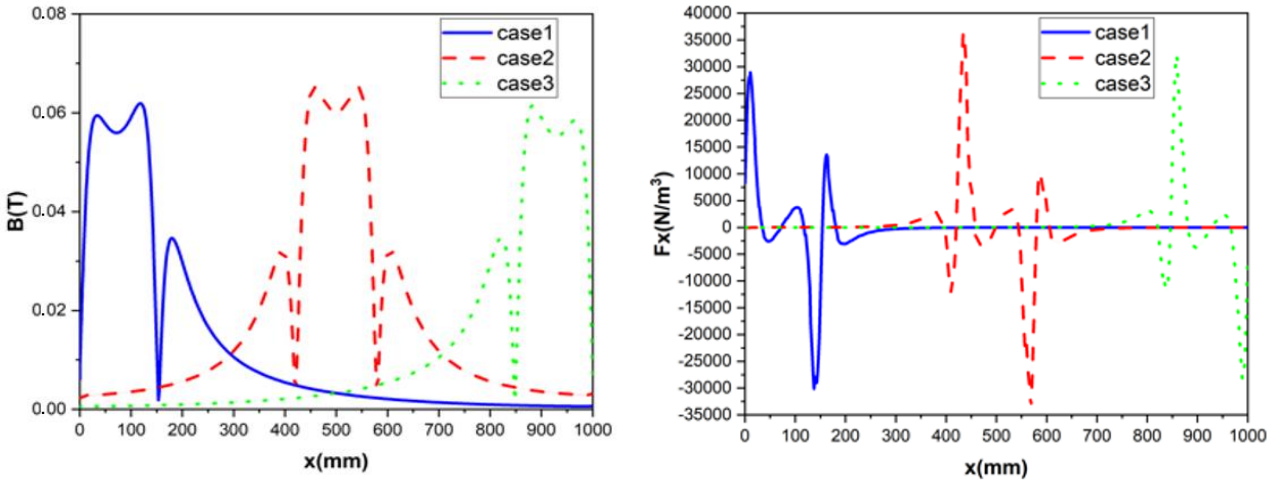

(a) **(b)**

Figure 6. Effect of the position of the magnet on the (a) magnetic flux density, and (b) Kelvin force.

Figure 7 shows how the velocity and streamlines of Fe_3O_4/water FF are affected by the position of the magnet in the channel. In case 1, when the magnet is located at the beginning of the channel, the flow is compressed and accelerated at the inlet, but a stable profile is quickly established downstream. When the magnet is located in the middle of the channel (case 2), more severe effects are observed, i.e., more severe distortions in the flow lines and recirculation zones, and stronger velocity gradients are created, indicating more mixing and greater heat transfer capacity. Finally, when the magnet is located at the outlet (case 3), the flow remains almost uniform throughout the channel, with only a few disturbances near the outlet, resulting in a relatively minor effect on the overall flow dynamics.

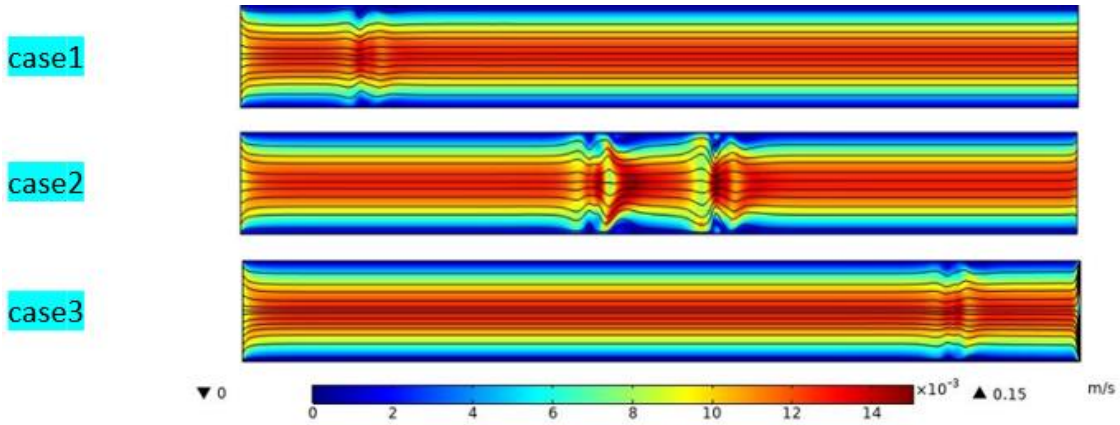

Figure 7. Effect of the position of the magnet on streamlines and velocity distribution.

Figure 8 shows the changes in the fluid velocity along the channel for different positions of the magnets. It can be observed that the velocity of FF under the MFs created near the magnets undergoes increasing and decreasing fluctuations ranging from 0.0075 m/s to 0.0153 m/s.

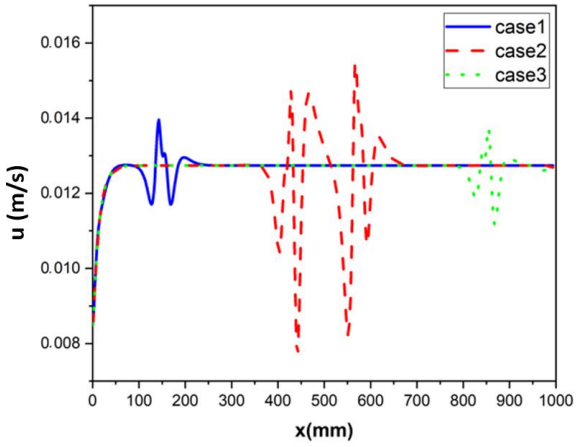

Figure 8. Changes in the velocity of ferrofluid on the cutline passing through the center of the channel, for different positions of the magnets.

It can be seen from Figure 8 that in case 2 (the magnet in the middle of the channel), the FF velocity fluctuated more, and the maximum velocity occurred in this case, which is consistent with the Kelvin force diagram.

Figure 9 shows the effect of the position of the magnet on the temperature distribution along the streamlines in the channel. Comparing Figures 7 and 9, it is observed that in regions where the fluid velocity increases, the fluid temperature decreases, and vice versa, in regions where the fluid velocity decreases, the temperature of that region increases. In case 1, the temperature of the fluid flow near the inlet increases due to the local magnetic interaction, but the fluid flow stabilizes rapidly downstream, resulting in a nearly uniform temperature gradient along the channel. In case 2, severe disturbances are observed in both the

temperature contours and the streamlines in the middle of the channel. The concentrated magnetic field in this region increases the turbulence of NP and, by increasing the fluid mixing, creates a more uniform temperature across the channel cross-section. This configuration offers the greatest potential for enhancing convective heat transfer. In case 3, disturbances in the temperature distribution are observed at the end of the channel, but a relatively stable temperature profile is observed in the bulk of the channel. As a result, a more limited impact on the overall heat transfer is seen compared to the same in case 2.

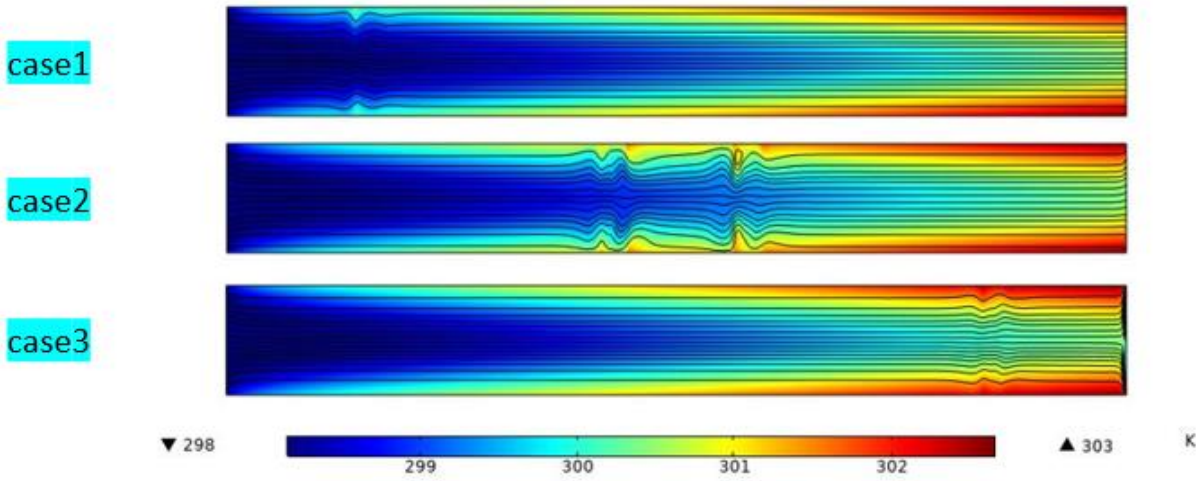

Figure 9. Effect of the position of the magnet on the temperature distribution and flow lines**.**

Figure 10 shows the changes in the local Nu along the channel. Nu fluctuates and increases locally in the presence of magnets and by increasing the MF intensity, but the overall Nu trend along the channel is decreasing due to the decrease in the temperature difference in the channel under a constant heat flux.

At the inlet, Nu has a maximum value of approximately 14–15 due to the developing thermal boundary layer. As the flow progresses downstream, Nu gradually decreases toward a fully developed value in all cases. According to Figure 10, it is observed that the local Nu is higher in case 2 than in the other cases.

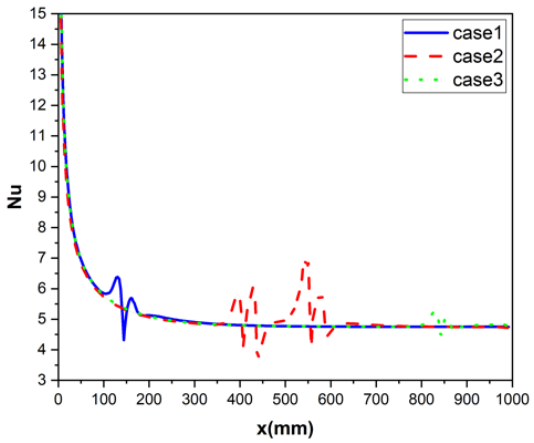

Figure 10. Effect of the position of the magnet on the local Nusselt number.

The percentage enhancement in the average Nu ($\overline{Nu}$), compared to the case without MF, for different cases is presented in Table 5. It is observed that $\overline{Nu}$ is higher in case 2 than in other cases.

Table 5.
Percentage increase in $\overline{Nu}$ for different cases compared to the case without MF.

Case	$\overline{Nu}$	Percentage enhancement (%)
1	5.29	0.40
2	5.31	0.68
3	5.28	0.34

6. Conclusions

In this study, a two-dimensional simulation of two magnets on the sides of a 1000 mm long channel under constant heat flux was performed. Three different magnet configurations were investigated (Mode 1, Mode 2, and Mode 3) in which the magnets were located at different distances from the channel entrance (the beginning, middle, and end of the channel). The effect of the distance and the position of the magnets along the channel on the MF intensity, Kelvin force, hydrodynamic behavior, and heat transfer was investigated. The results obtained are as follows:

- The location of the magnets and their distance from the entrance strongly affect the hydrodynamics of the flow and heat transfer.
- The presence of magnets around the channel affects the behavior of the flow and creates fluctuations in the fluid velocity at the location of MF in the fluid and near the magnets. The velocity fluctuations are caused by the Kelvin force fluctuations due to the interaction of the MF and NPs.
-When the magnet is located in the middle of the channel, the velocity fluctuations at the location of the magnets are greater, and the streamlines in this area show more turbulence. As a result, increasing the mixing across the channel causes temperature uniformity and improves convective heat transfer and Nu. When the magnets are placed at the beginning and end of the channel, only their local effects are observed.
- It is also observed that Nu fluctuates and increases locally in the presence of magnets and by increasing the MF intensity, but the overall Nu trend along the channel is decreasing due to the decrease in the temperature difference in the channel under a constant heat flux.
- When the magnet is located in the middle of the channel, the intensity of the magnetic field and also the Kelvin force values are the highest. Therefore, the location of the magnet in the middle of the channel will be the best suggestion for the heat dissipation of the channel fluid.

List of Symbols

B	Magnetic flux density [T]
B_r	Remnant magnetic flux density
C_p	Specific heat capacity [J/kgK]
D	Diameter of channel [m]
F	Kelvin force [N]
H	Magnetic field [A/m]
J	Electrical current density [A/r
k	Thermal conductivity [W/mK]
P	Pressure [Pa]
q''	Heat flux [W/m^2K]
T	Temperature [K]
u	Velocity [m/s]
X	Length [mm]

Greek symbols

μ	Dynamic Viscosity [$kg/m \cdot s$]
ρ	Density [kg/m^3]
φ	Volume fraction

Subscripts

bf	Base fluid
ff	Ferrofluid
out	Outlet
np	Nanoparticle

Non − dimensional numbers

Nu	Nusselt number $= h \cdot D/k$
Re	Reynolds number $= \rho u D/\mu$

Constants

μ_0	permeability of free space ($4\pi \times 10^{-7}$ H/m)

Abbreviations

FF	Ferrofluid
MF	Magnetic field
Nanofluid	NF
Nanoparticle	NP

References

[1] He Z, Yan Y, Zhang Z (2021) Thermal management and temperature uniformity enhancement of electronic devices by micro heat sinks: A review. Energy 216: 119223. https://doi.org/10.1016/j.energy.2020.119223

[2] Rostamian F, Etesami N, Haghgoo M (2021) Management of electronic board temperature using heat sink containing pure and microencapsulated phase change materials. International Communications in Heat and Mass Transfer 126: 105407. https://doi.org/10.1016/j.icheatmasstransfer.2021.105407

[3] Alhusseny A, Al-Aabidy Q, Al-Zurfi N, Nasser A, Aljanabi M (2021) Cooling of high-performance electronic equipment using graphite foam heat sinks. Applied Thermal Engineering 191: 116844. https://doi.org/10.1016/j.applthermaleng.2021.116844

[4] Kannan KG, Kamatchi R (2021) Experimental investigation on thermosyphon aid phase change material heat exchanger for electronic cooling applications. Journal of Energy Storage 39: 102649. https://doi.org/10.1016/j.est.2021.102649

[5] Dinarvand M, Abolhasani M, Hormozi F, Bahrami Z (2023) Experimental investigation and performance comparison of Fe_3O_4/water and $CoFe_2O_4$/water ferrofluids in presence of a magnetic field in a cooling system. Journal of the Taiwan Institute of Chemical Engineers 148: 104927. https://doi.org/10.1016/j.jtice.2023.104927

[6] Siricharoenpanich A, Wiriyasart S, Naphon P (2021) Study on the thermal dissipation performance of GPU cooling system with nanofluid as coolant. Case Studies in Thermal Engineering 25: 100904. https://doi.org/10.1016/j.csite.2021.100904

[7] Ghasemi SE, Ranjbar AA, Hosseini MJ (2017) Experimental evaluation of cooling performance of circular heat sinks for heat dissipation from electronic chips using nanofluid. Mechanics Research Communications 84: 85–89. https://doi.org/10.1016/j.mechrescom.2017.06.009

[8] Keshavarz F, Mirabdolah Lavasani A, Bayat H (2019) Numerical analysis of effect of nanofluid and fin distribution density on thermal and hydraulic performance of a heat sink with drop-shaped micropin fins. Journal of Thermal Analysis and Calorimetry 135: 1211–1228. https://doi.org/10.1007/s10973-018-7711-z

[9] Shyam S, Mehta B, Mondal PK, Wongwises S (2019) Investigation into the thermo-hydrodynamics of ferrofluid flow under the influence of constant and alternating magnetic field by infrared thermography. International Journal of Heat and Mass Transfer 135: 1233–1247. https://doi.org/10.1016/j.ijheatmasstransfer.2019.02.050

[10] Dinarvand M, Abolhasani M, Hormozi F, Bahrami Z (2023) Investigation of the effect of nanoparticle type on ferrofluid viscosity and its thermal performance in the presence and absence of a magnetic field: A new correlation. Journal of Magnetism and Magnetic Materials 587: 171270. https://doi.org/10.1016/j.jmmm.2023.171270

[11] Sheikholeslami M, Ganji DD, Rashidi MM (2015) Ferrofluid flow and heat

transfer in a semi-annulus enclosure in the presence of magnetic source considering thermal radiation. Journal of the Taiwan Institute of Chemical Engineers 47: 6–17. https://doi.org/10.1016/j.jtice.2014.09.026

[12] Sheikholeslami M, Hayat T, Alsaedi A (2017) Numerical study for external magnetic source influence on water based nanofluid convective heat transfer. International Journal of Heat and Mass Transfer 106: 745–755. https://doi.org/10.1016/j.ijheatmasstransfer.2016.09.077

[13] Karami E, Rahimi M, Azimi N (2018) Convective heat transfer enhancement in a pitted microchannel by stimulation of magnetic nanoparticles. Chemical Engineering and Processing: Process Intensification 126: 156–167. https://doi.org/10.1016/j.cep.2018.02.023

[14] Cunha LHP, Siqueira IR, Campos AAR, Rosa AP, Oliveira TF (2020) A numerical study on heat transfer of a ferrofluid flow in a square cavity under simultaneous gravitational and magnetic convection. Theoretical and Computational Fluid Dynamics 34: 119–132. https://doi.org/10.1007/s00162-020-00515-1

[15] Mehrez Z, El Cafsi A (2021) Heat exchange enhancement of ferrofluid flow into rectangular channel in the presence of a magnetic field. Applied Mathematics and Computation 391: 125634. https://doi.org/10.1016/j.amc.2020.125634

[16] Larimi MM, Ghanaat A, Ramiar A, Ranjbar AA (2016) Forced convection heat transfer in a channel under the influence of various non-uniform transverse magnetic field arrangements. International Journal of Mechanical Sciences 118: 101–112. https://doi.org/10.1016/j.ijmecsci.2016.09.023

[17] Benos LT, Polychronopoulos ND, Mahabaleshwar US, Lorenzini G, Sarris IE (2021) Thermal and flow investigation of MHD natural convection in a nanofluid-saturated porous enclosure: An asymptotic analysis. Journal of Thermal Analysis and Calorimetry 143: 751–765. https://doi.org/10.1007/s10973-019-09165-w

[18] Soltanipour H (2020) Two-phase simulation of magnetic field effect on the ferrofluid forced convection in a pipe considering Brownian diffusion, thermophoresis, and magnetophoresis. European Physical Journal Plus 135: 1–23. https://doi.org/10.1140/epjp/s13360-020-00725-w

[19] Nessab W, Kahalerras H, Fersadou B, Hammoudi D (2019) Numerical investigation of ferrofluid jet flow and convective heat transfer under the influence of magnetic sources. Applied Thermal Engineering 150: 271–284. https://doi.org/10.1016/j.applthermaleng.2018.12.164

[20] Xu H, Li Y, Zhang R, Zheng X, Chen L, Ni M (2026) Numerical study of flow around a cold square cylinder at low Reynolds number under a strong transverse magnetic field. International Journal of Heat and Mass Transfer 256: 128123. https://doi.org/10.1016/j.ijheatmasstransfer.2025.128123

[21] Ghafori H, Dehnavy MRA (2025) CFD simulation of heat transfer in a hot water channel with aluminum metal foam and magnetic fields. Applied Thermal Engineering 128669. https://doi.org/10.1016/j.applthermaleng.

2025.128669

[22] Faghani A, Mansourpour Z, Yavari M (2025) An investigation on the effect of magnetic field on induced fluid flow and heat transfer using CFD-DEM. Journal of Chemical and Petroleum Engineering. https://doi.org/10.22059/jchpe.2025.388308.1591

[23] Sheikholeslami M, Rokni HB (2017) Simulation of nanofluid heat transfer in presence of magnetic field: A review. International Journal of Heat and Mass Transfer 115: 1203–1233. https://doi.org/10.1016/j.ijheatmasstransfer.2017.08.108

[24] Dinarvand M, Abolhasani M, Hormozi F, Bahrami Z (2023) Effects of magnetic field gradient on heat transfer and irreversibility in a channel. Chemical Engineering Communications 210: 698–715. https://doi.org/10.1080/00986445.2021.1977927

[25] Fadaei F, Shahrokhi M, Molaei Dehkordi A, Abbasi Z (2017) Heat transfer enhancement of Fe_3O_4 ferrofluids in the presence of magnetic field. Journal of Magnetism and Magnetic Materials 429: 314–323. https://doi.org/10.1016/j.jmmm.2017.01.046

[26] Asfer M, Mehta B, Kumar A, Khandekar S, Panigrahi PK (2016) Effect of magnetic field on laminar convective heat transfer characteristics of ferrofluid flowing through a circular stainless steel tube. International Journal of Heat and Fluid Flow 59: 74–86. https://doi.org/10.1016/j.ijheatfluidflow.2016.01.009

[27] Sheikholeslami M, Gorji-Bandpay M, Ganji DD (2012) Magnetic field effects on natural convection around a horizontal circular cylinder inside a square enclosure filled with nanofluid. International Communications in Heat and Mass Transfer 39: 978–986. https://doi.org/10.1016/j.icheatmasstransfer.2012.05.020

[28] Brinkman HC (1952) The viscosity of concentrated suspensions and solutions. Journal of Chemical Physics 20: 571. https://doi.org/10.1063/1.1700493

[29] Gupta M, Singh V, Kumar R, Said Z (2017) A review on thermophysical properties of nanofluids and heat transfer applications. Renewable and Sustainable Energy Reviews 74: 638–670. https://doi.org/10.1016/j.rser.2017.02.073

[30] Dinarvand M, Abolhasani M, Hormozi F, Bahrami Z (2022) Cooling capacity of magnetic nanofluid in presence of magnetic field based on first and second laws of thermodynamics analysis. Energy Sources, Part A: Recovery, Utilization, and Environmental Effects 44: 7825–7840. https://doi.org/10.1080/15567036.2021.1872746

[31] Hong SH, Hrnjak PS (1999) Heat transfer in thermally developing flow of fluids with high Prandtl numbers preceding and following U-bend. Air Conditioning and Refrigeration Center Report CR-24.